

Electrical Tomography Sensor Modelling for Detection of Fuel Proportion in Vessel

Rian Fahrizal¹, Jaga Sobar Julianto¹, Alief Maulana¹, Rocky Alfanz¹, Ceri Ahendyarti¹, Rohmadi²,
Imamul Muttakin¹

¹ Universitas Sultan Ageng Tirtayasa, Jl. Jendral Soedirman KM. 3, Cilegon 42435, Indonesia

² C-Tech Labs Edwar Technology, Jl. KH Hasyim Ashari 79A, Tangerang 15141, Indonesia

ARTICLE INFO

Article history:

Received May 30, 2023

Revised June 30, 2023

Published July 03, 2023

Keywords:

Electrical tomography;
ECVT;
Sensor modelling;
Multiphysics simulation;
Linear back projection

ABSTRACT

Electrical capacitance volume tomography (ECVT) is a method for determining the volumetric distribution of dielectric permittivity using the capacitance measurement principle. The determination of volumetric distribution of dielectric permittivity is important to regulate a process in which quantity of materials is a decisive parameter such as in industrial setting or vehicle sub-system. ECVT is a relatively fast and non-radiating method to observe spatio-temporal phenomena inside a process, making it a valuable technique. Sensor modelling and image reconstruction study are essentials in designing a suitable imaging system based on measurements from plurality of electrodes providing higher degree of information being observed. This research conducts sensor modelling with varying fuel objects in the interior of a cylindrical vessel. The capacitance value was simulated between a combination of eight electrodes mounted encapsulating the tube. Each measured electrode was given an excitation voltage as a source of an electrostatic field, which interacts with the object's presence. The objects in this study are benzene, kerosene, and diesel fuel, along with reference dielectric values of water and air. Image reconstruction used the linear back projection (LBP) method. Matrix operations between sensor's pre-defined sensitivity and capacitance values produce data that can be plotted into an image estimating the true distribution of objects. Capacitance values from modelling are proportional to the actual object's permittivity. The reconstruction provides qualitative information on the proportion of fuel in the vessel based on the capacitance value. Images have distinct values according to the presence of different objects under investigation. The research contribution is a proof of concept in using capacitance tomography to detect different fuels inside an enclosed tank at modelling stage. In addition, this study serves as a guideline for implementing a non-invasive and non-intrusive system for determining proportions of materials of interests inside a certain setup.

This work is licensed under a [Creative Commons Attribution-Share Alike 4.0](https://creativecommons.org/licenses/by-sa/4.0/)



Corresponding Author:

Imamul Muttakin, Universitas Sultan Ageng Tirtayasa, Jl. Jendral Soedirman KM. 3, Cilegon 42435, Indonesia

Email: imamul@untirta.ac.id

1. INTRODUCTION

Tomography is a system or tool that sees the inside of an object in the form of slices (pieces) [1]. As a technology, tomography can describe objects quickly and easily. Besides, it can also provide complete information describing the object's state. Completeness of information is obtained by increasing the amount of information described in the structure of psychological objects, both internal and external structures, such as temperature, moisture content, and others. With these advantages, tomography has been widely developed, especially in the industrial and medical fields [2].

In the medical field, tomography is closely related to imaging technology used for diagnosing diseases before surgery; therefore, it is essential. The need to see the inside of objects on the human body is carried out non-invasively (without damaging) and non-intrusively (without inserting tools) [3]. The basic principle of tomography is that the patient is scanned by administering radiation energy, and then the energy interaction with the patient's body is measured. There are several techniques in medical imaging, and each has its characteristics. For instance, X-ray imaging shoots an X-ray source through the patient's body while placing a film behind it during exposure. Other medical imaging techniques commonly used in clinical settings comprise computed tomography (CT), magnetic resonance imaging (MRI), and ultrasound imaging. Almost all of those modern tomography techniques incorporate projected data from multiple directions and feed these data into a computerized tomographic reconstruction process [4].

Process tomography is a term for tomography applications in industrial fields [5]. Instead of static human body scanning, process tomography attempts to provide both spatial and temporal variation inside industrial processes such as multi-phase flow, mixing, separation, etc [6]-[8]. Certain radiation energy used are sensitive to different substances that exist in pipeline flow so that different phases in a flow e.g. water, oil, and gas can be investigated. Furthermore, a mixing process involves various materials altogether to achieve homogeneous mixture that need to be quantified. On the other hand, a crude oil extraction requires monitoring of separation degree to check its yields. Those characteristics demand fast imaging systems without nuclear radiation and not disturbing processes [9]. Electrical tomography uses a low-intensity field as an excitation energy to convey information in the region of interest (ROI) through passive electromagnetic properties measurements via a boundary sensing system. Boundary measurements could be resistive [10], capacitive [11], or inductive [12] systems depending on ROI characteristics. Those techniques have found areas of implementation in oil and gas [13]-[14], pharmacy [15]-[16], as well as food sectors [17].

However, challenges for electrical tomography deployment remain a work in progress by both researchers and industrial technicians. Improvement is sought in sensor design [18], hardware electronics [19]-[24], as well as image reconstruction algorithms [25]-[26]. In hardware measurement, the sensitivity and response time are among crucial aspects in order to catch the dynamic process monitoring. Meanwhile imperfection in image reconstruction affects the accuracy in quantifying the object. Particularly for sensor development, proper modelling has to be done to suit the target process, which varies from one implementation to another [27]. That is also the case with the difference in vessel's shape and object's distribution. This research conducts sensor modelling for a capacitive tomography system to determine fuel proportion in a tank. The capability is desirable in various designs that require an informed decision based on fuel storage or combusting substance, such as in refinery/reservoir, automobile, aviation, spacecraft, etc.

This paper explains sensor modelling work in the following fashion. The following section describes an overview of the capacitance tomography method, the image reconstruction algorithm used, and the post-processing step. The objects under study are benzene, kerosene, and diesel, which are commonly used fuels. The result section will show sensor design, output from sensor simulation and imaging analysis. The last section concludes this report and exposes its limitation while proposing further potential research. The research contribution is a proof of concept in using capacitance tomography to detect different fuels inside an enclosed tank at modelling stage. In addition, this study serves as a guideline for implementing a non-invasive and non-intrusive system for determining proportions of materials of interests inside a certain setup.

2. METHODS

Electrical capacitance volume tomography (ECVT) is a method for determining the volumetric distribution of the dielectric permittivity of objects in the interior covered by the sensor using the principle of capacitance measurement. The term ECVT was proposed by Warsito et al. in 2007 [28] following their first idea, which was developed in 2003 [29]. The ECVT principle is slightly different from tomography techniques in general. ECVT is not based on line projections but on volumetric capacitance measurement of the entire three-dimensional medium covered by the capacitance sensor. The three-dimensional space, which is the measured domain in ECVT, also does not have to be cylindrical like in existing tomography systems but can be an arbitrary shape or even an open space that can be reached by the static electric field created by the electrodes of the sensor which can be made in various forms.

Fig. 1 illustrates the components of the ECVT system. It consists of sensors, electronics, and computing devices. The Sensor system is constructed from an array of capacitive electrodes encapsulating the ROI. Each pair of electrodes could measure the capacitance dependent on material distribution in between. Whenever an object with electrical permittivity exists inside the domain, the calculated capacitance value will convey information about the object in question. The number of electrodes in the array affects the spatial resolution of the imaging result. Nevertheless, too many electrodes will deter the signal-to-noise ratio of the measurement.

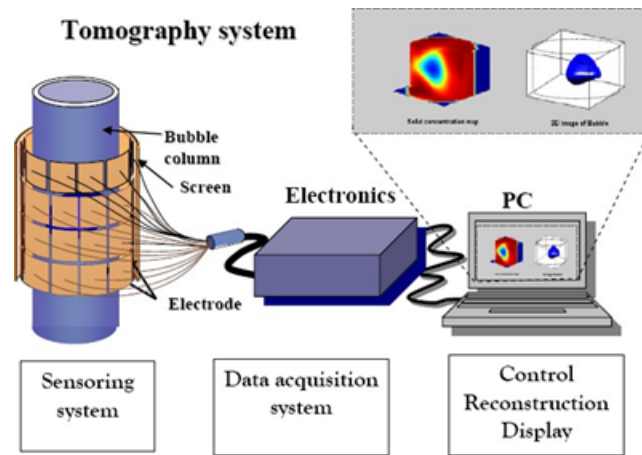


Fig. 1. Overview of an ECVT system [28]

This research uses the COMSOL Multiphysics software to do the sensor modelling. In COMSOL 3D domain, AC/DC module is used with electrostatic interface to solve stationary system. Having designed a proper geometry for the system, domains and boundaries are assigned to represent the actual physical configuration. For a capacitive system, an initial voltage is set at one electrode while the other electrodes are zeroed. Subsequently, running the simulation will result in electric field computation. Evaluating the specific boundary parts, quantity of interest can be derived. Simulations are carried out to obtain capacitance values that will be processed to produce images. Distribution of benzene, kerosene, and diesel fuel objects will be used for the simulation. After getting the capacitance value, the data is logged into the microcontroller. MATLAB interface will be built to retrieve data stored on the microcontroller so that it can be imaged.

A complex electronics system which usually perform measurement's signal conditioning and acquisition was replaced by a simplified data storage and interfacing using microcontroller platform. This approach ensures interoperability for the developed model to be used with another hardware platform. Industrial plant usually has its own dedicated hardware and/or control system. Therefore, a common storage and interfacing will make the sensor model easily adapted into the existing setup. A detailed electronic design is the subject of another work and has been reported, for example, in [30]-[32]. At the end of the process, image reconstruction will be analyzed for qualitative objects' appearance and compared with valid permittivity values.

Linear back projection (LBP) is one of the first algorithms to reconstruct images from capacitance boundary measurement [33]. This algorithm is still commonly used as a capacitance-based tomographic reconstruction technique. This algorithm is based on the assumption that the sensitivity value is constant within the sensing space. In addition, the sensitivity is assumed to be the same for the various region of interest.

The algorithm uses the relationship between the measured capacitance and the image. A sensitivity function S is derived to find an image vector G based on the estimated C capacitance vector. This method is an approximation method represented in the following equation:

$$C = SG \quad (1)$$

This equation has a solution to get a $G_{[N \times 1]}$ image by inner product between $C_{[M \times 1]}$ and the inverted sensitivity $G_{[M \times N]}$ as:

$$G = S^{-1}C \quad (2)$$

In practice, the inverse of S , as in (2), is usually undefined, so a matrix approximation is used. The LBP algorithm uses the transpose value of the sensitivity matrix instead of its inverse, so it has a dimension of $[N \times M]$. The scheme of the LBP method is shown in Fig. 2.

Therefore, the image element is obtained from the following:

$$G = S^T C \quad (3)$$

$$G(x, y, z) = S^T(x, y, z) \sum_i^{Ne} \sum_j^{Ne} \frac{C_{i,j}^{meas} - C_{i,j}^{empty}}{C_{i,j}^{full} - C_{i,j}^{empty}} \quad (4)$$

Where C_{meas} is the measured capacitance between electrodes i and j , C_{empty} is the capacitance between electrode pairs i and j when material permittivity in the measurement area is low, whereas C_{full} is the

capacitance between electrodes i and j when the measurement area is given a high permittivity material. Here, N_e is the number of electrodes [3]. For N_e number of electrodes, there can be a total of $N_e(N_e - 1)/2$ independent measurement combination M .

The reconstruction process of the LBP method refers to (3), which is to find the value of G (N pixels) from the measured capacitance value C (from sensor measurements taken by the modelling in the form of a matrix) and the sensitivity value of the S matrix. The sensitivity matrix defines the change of measured value against the change of object interaction in a discrete region (or image pixel). This matrix can be derived using prior computation [34].

As shown in Fig. 3, capacitance values obtained from the sensor can be processed using (4) in the form of normalized C , which is the measured object's capacitance value relative against known references of air (as 'empty' condition) and water (as 'full' condition) according to right hand side of (4). S is the sensitivity value on the sensor, and G is the reconstructed image. The pixelated image (32×32) is obtained by matrix multiplication between transposed sensitivity and capacitance values.

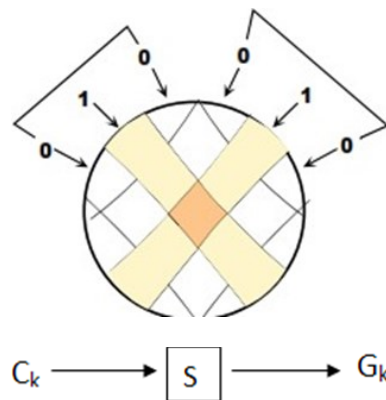


Fig. 2. Back projection mechanism

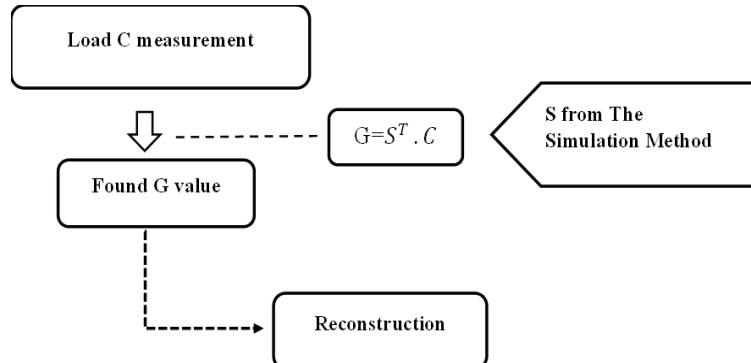


Fig. 3. Post-processing measurement data into the image using LBP

3. RESULTS AND DISCUSSION

The sensor is a device for detecting the interaction between energizing field and material distribution in the ROI. For electrode plate systems, the dielectric material disturbs the electric fields resulting in capacitance quantities to be sensed. These measured values, in turns can be processed into an image representing the original dielectric distribution.

Referring to Fig. 4 (left), the sensor consists of 8 electrodes/channels (S) encircling a tube with a height of 10 cm and a diameter of 12 cm. Each electrode has a length of 8 cm and a width of 4 cm. The material used in the sensor consists of copper as an electrode with polymers as a frame. Inside the sensor, there will be objects (O) to be placed for the modelling. Fig. 4 (center) shows the sensor and object having been meshed for finite element electromagnetic simulation in COMSOL. Free tetrahedral mesh was applied in this simulated geometry. Electric field lines emitting from the activated electrode are illustrated in Fig. 4 (right).

The object in question is a material that will be contained in the sensor tube, which will then be processed into an image. In this study, the objects are kerosene, benzene, and diesel fuel. Table 1 lists the relative permittivity values of each material [35]. Kerosene has a permittivity value of 1.8 F/m, diesel fuel has a permittivity value of 2.1 F/m, and benzene has a permittivity value of 2.3 F/m. Additionally, the reconstruction

process requires reference data with an object in the form of water with a permittivity value of 80.1 F/m (upper limit) and without an object (air) with a permittivity value of 1 F/m (lower limit). Consequently, image values are normalized respective to those references [36].

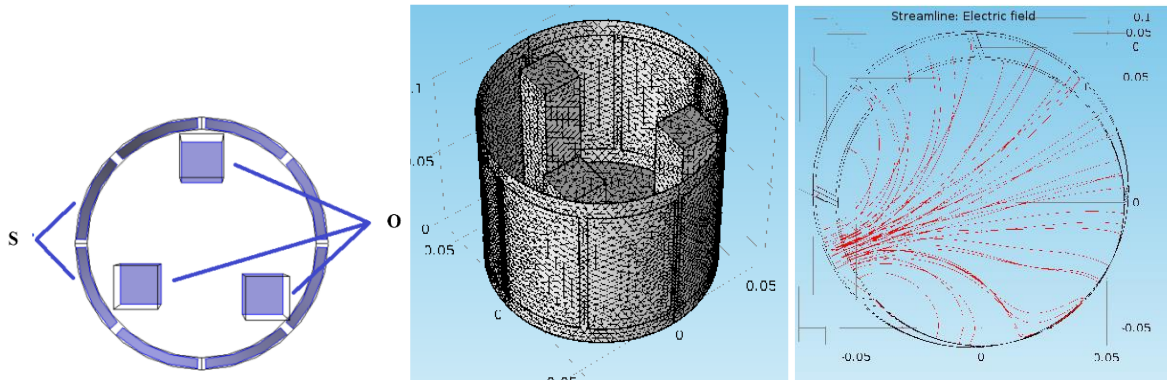


Fig. 4. Sensor modelling and multiphysics simulation

Table 1. Permittivity of Materials

Material	Relative Permittivity (F/m)
Air	1
Water	80.1
Kerosene	1.8
Diesel	2.1
Benzene	2.3

For the abovementioned cases, data collection is done by providing an excitation voltage of 5 V on one active electrode and measuring transmission parameters from the rest of the electrodes. The simulated measurement data is in the form of capacitance values from the combination of channel pairs so that 28 values are obtained. Fig. 5 shows capacitance values measured between simulated electrodes. On the x-axis is the measurement index representing electrode pairs combination, i.e., index 0 for pairing between electrode one and electrode 2, index 1 for pairing between electrode one and electrode 3, and so forth up to index 27 for pairing between electrode seven and electrode 8. Adjacent electrode pairs gives higher capacitance value than opposite electrode pairs due to capacitance is inversely proportional to the distance between electrodes.

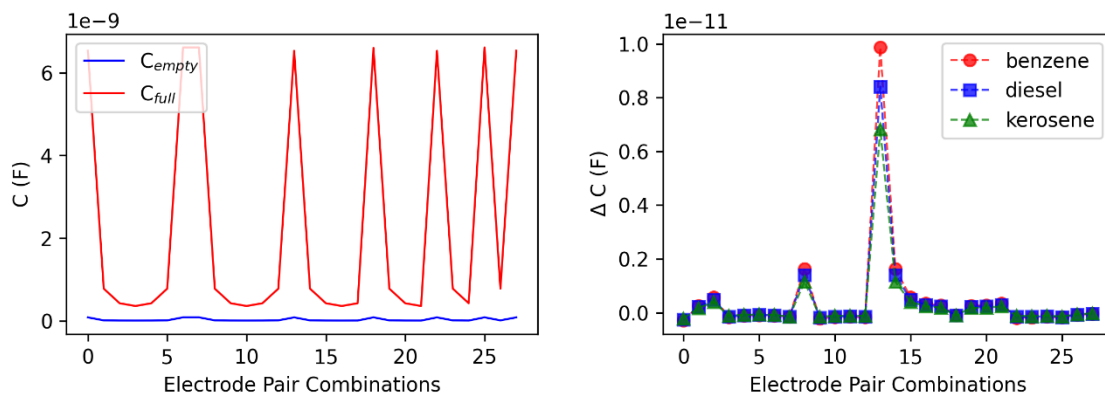


Fig. 5. Plot of measured capacitance for reference (left) and the change caused by objects (right)

Both upper limit (water object) and lower limit ('empty' air space) plots are depicted in Fig. 5 (left). After placing a single object, the difference between 'empty' values and measured (with different objects) values are plotted in Fig. 5 (right). For particular electrode pairs where the object is placed nearby, the values show a proper level according to the permittivity of objects, starting from the lowest (kerosene) to diesel, to the highest (benzene).

In addition, the proportionality of the simulation values is also analyzed. For each fuel object, all capacitance difference values given by electrode-pairs measurement are aggregated using the L_2 norm. This

operation ensures that every boundary measurement from electrodes is considered. The resulting value is then plotted against the true permittivity value. Fig. 6 shows that the simulation values are proportional to the permittivity values as indicated by an incrementally consistent line plot.

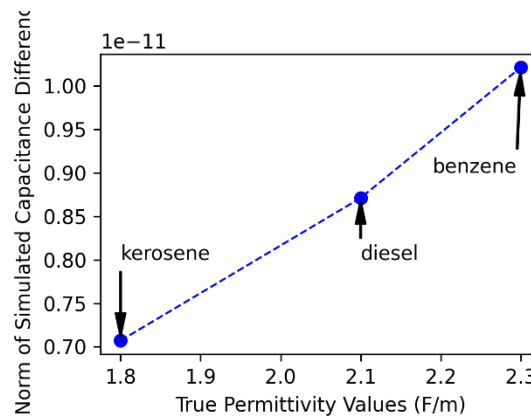


Fig. 6. Norm of simulated capacitance difference against object's true permittivity values

After the above data is processed using (4), the LBP operation is computed in MATLAB. The resulting 2-dimensional matrix can be plotted as an image section showing objects' distribution. Fig. 7 shows a single benzene fuel object placed in the north, viewing from the top of the vessel. Fig. 8 shows two diesel fuel objects placed in the north and southeast, viewing from the top of the vessel. Fig. 9 shows three kerosene fuel objects placed in the north, southeast, and southwest, viewing from the top of the vessel.

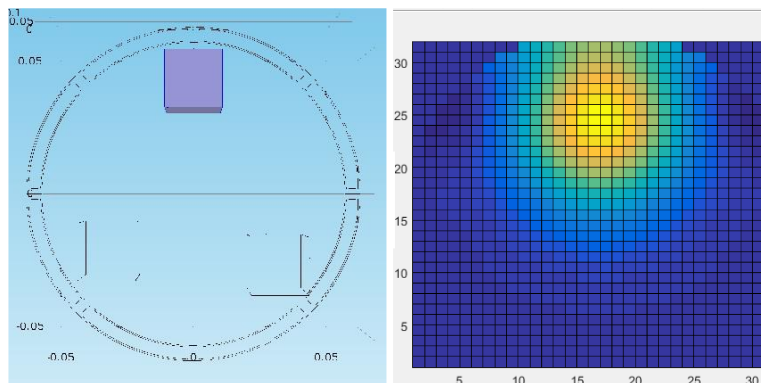


Fig. 7. The reconstructed image of one object (benzene)

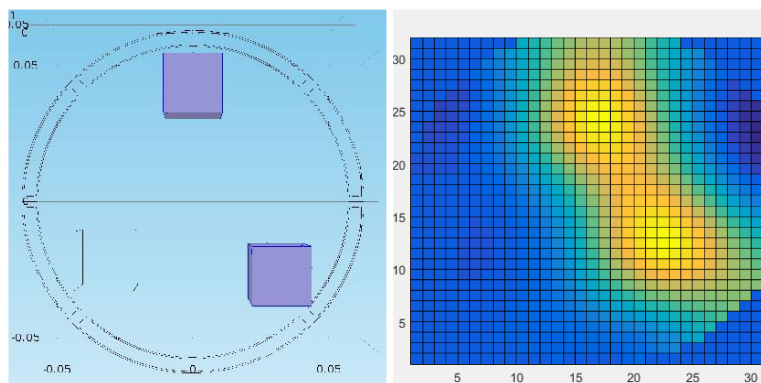


Fig. 8. The reconstructed image of two objects (diesel)

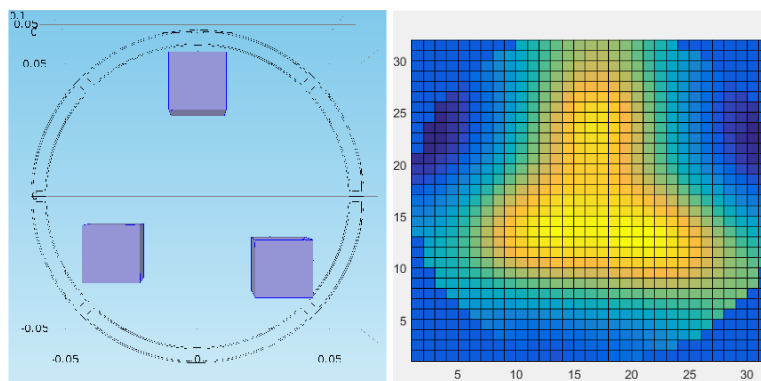


Fig. 9. The reconstructed image of three objects (kerosene)

The reconstruction results are shown on the left-hand side of each Fig. 7 to Fig. 9. Normalized values illustrated in the pixelated image section are represented by blue (low) to yellow (high) colors. For a single object in Fig. 7, the object is depicted quite clearly regarding its location and prominence against the remaining pixels in the ROI. However, the object's shape is obscure in the sense that a true square-shaped object turns into a round-shaped image. In Fig. 8, two objects are reconstructed according to their location, but the separation between them are not distinctive. And in the case of three objects (Fig. 9), each object's image is pulled to the centre, although the corners still indicate their true locations. Those blur and expansion are among the drawbacks of the LBP algorithm.

Some improvements in the image reconstruction algorithm have been investigated. Sophisticated methods involving deep learning are reported [37]-[40]. Nevertheless, they come with another issue such as longer reconstruction time which hinder the desired real-time feature of process tomography. Computational means also require hardware complexity which incurs implementation cost. Thus, for a particular target application, the low-cost and fast LBP algorithm is still sufficient.

4. CONCLUSION

Sensor modelling in the ECVT system has been investigated for the determination of fuel proportion in a vessel. The LBP reconstruction method for imaging provides results that can distinguish objects according to their permittivity values. In the reconstruction of one object, the blurring effect is visible around the image of the object. In the reconstruction of two and three objects, the image results appear to blend with one another. Simulation results show that objects with kerosene, diesel and benzene permittivity values can be observed proportionally. In order to optimize the reconstruction results, a larger number of electrodes and a smaller sensor size might produce high-resolution images. Meanwhile, other more complex algorithms are needed to obtain images with a close resemblance to true objects. The algorithm development can be directed to an iterative method with the aid of machine learning implementation.

REFERENCES

- [1] F. Wang, Q. Marashdeh, L.-S. Fan, and W. Warsito, "Electrical Capacitance Volume Tomography: Design and Applications," *Sensors*, vol. 10, no. 3, pp. 1890–1917, 2010, <https://doi.org/10.3390/s100301890>.
- [2] M. K. Arya, S. S. Kharor, R. Singh, and P. K. Singh, "A Low Cost Electrical Impedance Tomography Using EIDORS," *International Journal of Basic and Applied Biology*, vol. 2, no. 6, pp. 385–387, 2015, <https://www.krishisanskriti.org/ijbab.php?Id=216>.
- [3] Q. Marashdeh, W. Warsito, L.-S. Fan and F. L. Teixeira, "A Multimodal Tomography System Based on ECT Sensors," in *IEEE Sensors Journal*, vol. 7, no. 3, pp. 426–433, 2007, <https://doi.org/10.1109/JSEN.2006.890149>.
- [4] J. L. Hubers, A. C. Striegel, T. J. Heindel, J. N. Gray, and T. C. Jensen, "X-ray computed tomography in large bubble columns," *Chemical Engineering Science*, vol. 60, no. 22, pp. 6124–6133, 2005, <https://doi.org/10.1016/j.ces.2005.03.038>.
- [5] M. S. Beck and R. A. Williams, "Process tomography: a European innovation and its applications," *Meas. Sci. Technol.*, vol. 7, no. 3, pp. 215–224, 1996, <https://doi.org/10.1088/0957-0233/7/3/002>.
- [6] K. Hsin-Y. Wei, C.-H. Qiu, and K. Primrose, "Super-sensing technology: industrial applications and future challenges of electrical tomography," *Phil. Trans. R. Soc. A.*, vol. 374, no. 2070, p. 20150328, 2016, <https://doi.org/10.1098/rsta.2015.0328>.
- [7] J. Yao and M. Takei, "Application of Process Tomography to Multiphase Flow Measurement in Industrial and Biomedical Fields: A Review," in *IEEE Sensors Journal*, vol. 17, no. 24, pp. 8196–8205, 2017, <https://doi.org/10.1109/JSEN.2017.2682929>.

- [8] R. K. Rasel, S. M. Chowdhury, Q. M. Marashdeh, and F. L. Teixeira, "Review of Selected Advances in Electrical Capacitance Volume Tomography for Multiphase Flow Monitoring," *Energies*, vol. 15, no. 14, p. 5285, 2022, <https://doi.org/10.3390/en15145285>.
- [9] U. Hampel *et al.*, "A Review on Fast Tomographic Imaging Techniques and Their Potential Application in Industrial Process Control," *Sensors*, vol. 22, no. 6, p. 2309, 2022, <https://doi.org/10.3390/s22062309>.
- [10] C. C. Barber, B. H. Brown, and I. L. Freeston, "Imaging spatial distributions of resistivity using applied potential tomography," *Electron. Lett.*, vol. 19, no. 22, p. 933, 1983, <https://doi.org/10.1049/el:19830637>.
- [11] S. M. Huang, A. B. Plaskowski, C. G. Xie, and M. S. Beck, "Capacitance-based tomographic flow imaging system," *Electron. Lett.*, vol. 24, no. 7, p. 418, 1988, <https://doi.org/10.1049/el:19880283>.
- [12] Z. Z. Yu, A. T. Peyton, M. S. Beck, W. F. Conway, and L. A. Xu, "Imaging system based on electromagnetic tomography (EMT)," *Electron. Lett.*, vol. 29, no. 7, p. 625, 1993, <https://doi.org/10.1049/el:19930418>.
- [13] I. Ismail, J. C. Gamio, S. F. A. Bukhari, and W. Q. Yang, "Tomography for multi-phase flow measurement in the oil industry," *Flow Measurement and Instrumentation*, vol. 16, no. 2-3, pp. 145-155, 2005, <https://doi.org/10.1016/j.flowmeasinst.2005.02.017>.
- [14] L. S. Hansen, S. Pedersen, and P. Durdevic, "Multi-Phase Flow Metering in Offshore Oil and Gas Transportation Pipelines: Trends and Perspectives," *Sensors*, vol. 19, no. 9, p. 2184, 2019, <https://doi.org/10.3390/s19092184>.
- [15] F. Ricard, C. Brechtelsbauer, X. Y. Xu, and C. J. Lawrence, "Monitoring of Multiphase Pharmaceutical Processes Using Electrical Resistance Tomography," *Chemical Engineering Research and Design*, vol. 83, no. 7, pp. 794-805, 2005, <https://doi.org/10.1205/cherd.04324>.
- [16] H. Wang and W. Yang, "Application of electrical capacitance tomography in pharmaceutical fluidised beds – A review," *Chemical Engineering Science*, vol. 231, p. 116236, 2021, <https://doi.org/10.1016/j.ces.2020.116236>.
- [17] *Industrial Tomography*. Elsevier, 2015. <https://doi.org/10.1016/C2013-0-16466-5>.
- [18] W. Yang, "Design of electrical capacitance tomography sensors," *Meas. Sci. Technol.*, vol. 21, no. 4, p. 042001, 2010, <https://doi.org/10.1088/0957-0233/21/4/042001>.
- [19] A. Yusuf, I. Muttakin, Rohmadi, A. Rudin, W. Widada and W. P. Taruno, "Single signal conditioning multi electrode for ECVT data acquisition system," *TENCON 2014 - 2014 IEEE Region 10 Conference*, pp. 1-6, 2014, <https://doi.org/10.1109/TENCON.2014.7022280>.
- [20] A. Yusuf, I. Muttakin, W. Widada, and W. P. Taruno, "Analysis of single excitation signal for high speed ECVT data acquisition system," in *2014 6th International Conference on Information Technology and Electrical Engineering (ICITEE)*, pp. 1-6, 2014, <https://doi.org/10.1109/ICITEED.2014.7007953>.
- [21] I. Muttakin, A. Yusuf, R. Rohmadi, W. Widada, and W. P. Taruno, "Design and Simulation of Quadrature Phase Detection in Electrical Capacitance Volume Tomography," *TELKOMNIKA*, vol. 13, no. 1, p. 55, 2015, <https://doi.org/10.12928/telkomnika.v13i1.1299>.
- [22] A. Yusuf *et al.*, "Switch Configuration Effect on Stray Capacitance in Electrical Capacitance Volume Tomography Hardware," *TELKOMNIKA*, vol. 14, no. 2, p. 456, 2016, <https://doi.org/10.12928/telkomnika.v14i2.3328>.
- [23] M. I. Ikhsanti, R. Bouzida, S. K. Wijaya, Rohmadi, I. Muttakin, and W. P. Taruno, "Capacitance-digital and impedance converter as electrical tomography measurement system for biological tissue," in *1st International Symposium of Biomedical Engineering (ISBE)*, p. 040013, 2017, <https://doi.org/10.1063/1.4976798>.
- [24] M. Al-Hawari, A. I. Aulia, A. Rudin, Rohmadi, I. Muttakin, and W. P. Taruno, "Receiver Circuit Design for Signal Conditioning in Magnetic Induction Tomography System," in *2017 5th International Conference on Instrumentation, Communications, Information Technology, and Biomedical Engineering (ICICI-BME)*, pp. 1-6, 2017, <https://doi.org/10.1109/ICICI-BME.2017.8537732>.
- [25] W. Q. Yang and L. Peng, "Image reconstruction algorithms for electrical capacitance tomography," *Meas. Sci. Technol.*, vol. 14, no. 1, pp. R1-R13, 2003, <https://doi.org/10.1088/0957-0233/14/1/201>.
- [26] B. Chen, J. Abascal, and M. Soleimani, "Electrical Resistance Tomography for Visualization of Moving Objects Using a Spatiotemporal Total Variation Regularization Algorithm," *Sensors*, vol. 18, no. 6, p. 1704, 2018, <https://doi.org/10.3390/s18061704>.
- [27] F. N. Adiputri, E. N. Prasetyani, Rohmadi, A. Saputra, I. Muttakin, and W. P. Taruno, "Simulation of Magnetic Induction Tomography Sensor with 8-Coils Solenoid and Planar," in *2017 5th International Conference on Instrumentation, Communications, Information Technology, and Biomedical Engineering (ICICI-BME)*, pp. 1-5, 2017, <https://doi.org/10.1109/ICICI-BME.2017.8537753>.
- [28] W. Warsito, Q. Marashdeh and L. -S. Fan, "Electrical Capacitance Volume Tomography," in *IEEE Sensors Journal*, vol. 7, no. 4, pp. 525-535, 2007, <https://doi.org/10.1109/JSEN.2007.891952>.
- [29] W. Warsito and L.-S. Fan, "Neural network multi-criteria optimization image reconstruction technique (NN-MOIRT) for linear and non-linear process tomography," *Chemical Engineering and Processing: Process Intensification*, vol. 42, no. 8, pp. 663-674, 2003, [https://doi.org/10.1016/S0255-2701\(02\)00204-0](https://doi.org/10.1016/S0255-2701(02)00204-0).
- [30] A. Yusuf *et al.*, "Circuit and Signal Processing for Capacitance Measurement of Breast Tissue," *Adv Sci Engng Med*, vol. 7, no. 10, pp. 900-905, 2015, <https://doi.org/10.1166/asem.2015.1779>.
- [31] I. Muttakin and M. Soleimani, "Direct capacitance measurement for tomographic imaging of metallic object." In *9th World Congress in Industrial Process Tomography*, pp. 509-514, 2018, <https://www.isipt.org/world-congress/9/29260.html>.
- [32] R. Alfanz, M. Fauzi, I. Muttakin, R. Fahrizal and Y. Okazaki, "Low-cost Impedance Measurement System for Determination of Condition and Oil Content in Wood Material," *2022 International Conference on Informatics Electrical and Electronics (ICIEE)*, pp. 1-4, 2022, <https://doi.org/10.1109/ICIEE55596.2022.10009989>.

- [33] H. Herdian, I. Muttakin, A. Saputra, A. Yusuf, W. Widada and W. P. Taruno, "Hardware implementation of linear back-projection algorithm for capacitance tomography," *2015 4th International Conference on Instrumentation, Communications, Information Technology, and Biomedical Engineering (ICICI-BME)*, pp. 124-129, 2015, <https://doi.org/10.1109/ICICI-BME.2015.7401348>.
- [34] D. N. Dyck, D. A. Lowther, and E. M. Freeman, "A method of computing the sensitivity of electromagnetic quantities to changes in materials and sources," *IEEE Trans. Magn.*, vol. 30, no. 5, pp. 3415-3418, 1994, <https://doi.org/10.1109/20.312672>.
- [35] K. F. Young and H. P. R. Frederikse, "Compilation of the Static Dielectric Constant of Inorganic Solids," *Journal of Physical and Chemical Reference Data*, vol. 2, no. 2, pp. 313-410, 1973, <https://doi.org/10.1063/1.3253121>.
- [36] S. Chowdhury, Q. M. Marashdeh, and F. L. Teixeira, "Inverse Normalization Method for Cross-Sectional Imaging and Velocimetry of Two-Phase Flows Based on Electrical Capacitance Tomography," *IEEE Sens. Lett.*, vol. 2, no. 1, pp. 1-4, 2018, <https://doi.org/10.1109/LESENS.2018.2806845>.
- [37] O. Costilla-Reyes, P. Scully, and K. B. Ozanyan, "Deep Neural Networks for Learning Spatio-Temporal Features From Tomography Sensors," *IEEE Trans. Ind. Electron.*, vol. 65, no. 1, pp. 645-653, 2018, <https://doi.org/10.1109/TIE.2017.2716907>.
- [38] J. Zheng, J. Li, Y. Li, and L. Peng, "A Benchmark Dataset and Deep Learning-Based Image Reconstruction for Electrical Capacitance Tomography," *Sensors*, vol. 18, no. 11, p. 3701, 2018, <https://doi.org/10.3390/s18113701>.
- [39] G. Wang, J. C. Ye, and B. De Man, "Deep learning for tomographic image reconstruction," *Nat Mach Intell*, vol. 2, no. 12, pp. 737-748, 2020, <https://doi.org/10.1038/s42256-020-00273-z>.
- [40] J. Li, D. Hu, W. Chen, Y. Li, M. Zhang, and L. Peng, "CNN-Based Volume Flow Rate Prediction of Oil-Gas-Water Three-Phase Intermittent Flow from Multiple Sensors," *Sensors*, vol. 21, no. 4, p. 1245, 2021, <https://doi.org/10.3390/s21041245>.

BIOGRAPHY OF AUTHORS

Rian Fahrizal

Email: rian.fahrizal@untirta.ac.id

Jaga Sobar Julianto

Email: jaga.sobar.julianto@gmail.com

Alief Maulana

Email: masaliefftuntirta@gmail.com

Rocky Alfanz

Email: rocky.alfanz@untirta.ac.id

Ceri Ahendyarti

Email: ceri.ahend@untirta.ac.id

Rohmadi

Email: rohmedi@c-techlabs.com

Imamul Muttakin

Email: imamul@untirta.ac.id

Orcid: 0000-0002-8409-4942